



Fischer, R. A., Campbell, A. J., Lord, O. T., Shofner, G. A., Dera, P., & Prakapenka, V. B. (2011). Phase transition and metallization of FeO at high pressures and temperatures. *Geophysical Research Letters*, 38(24), 1-5. [L24301]. [10.1029/2011GL049800](https://doi.org/10.1029/2011GL049800)

Publisher's PDF, also known as Final Published Version

Link to published version (if available):  
[10.1029/2011GL049800](https://doi.org/10.1029/2011GL049800)

[Link to publication record in Explore Bristol Research](#)  
PDF-document

## University of Bristol - Explore Bristol Research

### General rights

This document is made available in accordance with publisher policies. Please cite only the published version using the reference above. Full terms of use are available:  
<http://www.bristol.ac.uk/pure/about/ebr-terms.html>

### Take down policy

Explore Bristol Research is a digital archive and the intention is that deposited content should not be removed. However, if you believe that this version of the work breaches copyright law please contact [open-access@bristol.ac.uk](mailto:open-access@bristol.ac.uk) and include the following information in your message:

- Your contact details
- Bibliographic details for the item, including a URL
- An outline of the nature of the complaint

On receipt of your message the Open Access Team will immediately investigate your claim, make an initial judgement of the validity of the claim and, where appropriate, withdraw the item in question from public view.

## Phase transition and metallization of FeO at high pressures and temperatures

Rebecca A. Fischer,<sup>1</sup> Andrew J. Campbell,<sup>1</sup> Oliver T. Lord,<sup>2</sup> Gregory A. Shofner,<sup>3</sup> Przemyslaw Dera,<sup>4</sup> and Vitali B. Prakapenka<sup>4</sup>

Received 29 September 2011; revised 27 October 2011; accepted 1 November 2011; published 16 December 2011.

[1] Wüstite,  $\text{Fe}_{1-x}\text{O}$ , is an important component in the mineralogy of Earth's lower mantle and may also be a component of the core. Therefore its high pressure-temperature behavior, including its electronic structure, is essential to understanding the nature and evolution of Earth's deep interior. We performed X-ray diffraction and radiometric measurements on wüstite in a laser-heated diamond anvil cell, finding an insulator-metal transition at high pressures and temperatures. Our data show a negative slope for this apparently isostructural phase boundary, which is characterized by a volume decrease and emissivity increase. The metallic phase of FeO is stable at conditions of the lower mantle and core, which has implications for the high  $P$ - $T$  character of Fe-O bonds, magnetic field propagation, and lower mantle conductivity. **Citation:** Fischer, R. A., A. J. Campbell, O. T. Lord, G. A. Shofner, P. Dera, and V. B. Prakapenka (2011), Phase transition and metallization of FeO at high pressures and temperatures, *Geophys. Res. Lett.*, 38, L24301, doi:10.1029/2011GL049800.

### 1. Introduction

[2] Wüstite,  $\text{Fe}_{1-x}\text{O}$ , is an important endmember of (Mg,Fe)O in the Earth's lower mantle and possibly also a significant alloying component of the core [McDonough, 2003]. Its electronic structure at high pressures and temperatures contributes to the thermal and electrical conductivity of the lower mantle, stability of ferropericlase, and magnetic field propagation. It has recently been proposed that some pockets of the lowermost mantle are extremely enriched in FeO [Wicks *et al.*, 2010], enhancing these contributions. If oxygen is a primary light element component in the core, the nature of the Fe-O bond at high  $P$ - $T$  conditions may control oxygen solubility and partitioning in the core, and may also reflect the properties of a liquid Fe-O outer core. Therefore it is essential to understand the high pressure, high temperature electronic behavior of the Fe-O system. In this study we report on the stability of a metallic phase of wüstite, whose presence in the lower mantle and core could change our understanding of geochemical and geophysical processes in the deep Earth.

[3] The phase diagram of wüstite has been appropriately described as "enigmatic" [Mao *et al.*, 1996]. Under ambient

conditions it is stable in the B1 (NaCl-type) crystal structure. With room temperature compression it undergoes a rhombohedral  $R\bar{3}$  [Mao *et al.*, 1996] or monoclinic  $C2/m$  [Kantor *et al.*, 2008] symmetry distortion around 17 GPa, then transforms to the B8 (NiAs-type) crystal structure at higher pressures and moderate temperatures [Fei and Mao, 1994; Fischer *et al.*, 2011; Kondo *et al.*, 2004; Murakami *et al.*, 2004; Ozawa *et al.*, 2010a; Yagi *et al.*, 1988]. The B1 structure remains stable at higher temperatures, being the stable phase along the geotherm through the mantle and outer core [Fischer *et al.*, 2011; Ozawa *et al.*, 2010a]. The melting curve of  $\text{Fe}_{1-x}\text{O}$  has been determined up to pressures and temperatures of 77 GPa and 3100 K [Fischer and Campbell, 2010]. FeO also has interesting magnetic properties, with a transition from a paramagnetic to an antiferromagnetic state at  $\sim 20$  GPa with strong magnetoelastic coupling [Struzhkin *et al.*, 2001].

[4] Additionally, electrical resistivity measurements in diamond cell [Knittle and Jeanloz, 1991] and shock wave [Knittle *et al.*, 1986] experiments show a dramatic drop in resistivity in wüstite at high pressures and temperatures, and a reversal in the trend between temperature and resistivity, with the higher pressure phase showing a resistivity that decreases with increasing temperature. This electronic transition, interpreted as metallization, was initially thought to coincide with the B1-B8 transition, but with new constraints on the location and slope of the B1/B8 phase boundary [Fischer *et al.*, 2011; Kondo *et al.*, 2004; Ozawa *et al.*, 2010a], it has become apparent that this is not the case (Figure 1), causing confusion as to the nature of the metallization transition. Another recent study reported resistivity measurements on FeO in a diamond cell and found that B1-FeO is a semiconductor up to  $\sim 70$  GPa and 1760 K, while B8 FeO is metallic [Ohta *et al.*, 2010] (Figure 1). Theoretical studies predict metallization of B1-FeO at high pressures [Ringwood, 1977; Sherman, 1989], but the location of this transition has not been predicted. In this study, we reproduce the insulator/metal phase transition in wüstite and constrain the location and slope of this boundary using two different experimental methods, X-ray diffraction and radiometric techniques in the laser-heated diamond anvil cell, and investigate possible effects of non-stoichiometry on this phase boundary. A metallic phase of FeO at high  $P$ - $T$  conditions has implications for magnetic field propagation, lower mantle conductivity, stability of ferropericlase, and the nature of high  $P$ - $T$  Fe-O bonds.

### 2. Experimental Methods

[5] Materials and methods for the radiometric experiments are similar to those described by Fischer and Campbell

<sup>1</sup>Department of the Geophysical Sciences, University of Chicago, Chicago, Illinois, USA.

<sup>2</sup>Department of Earth Sciences, University College London, London, UK.

<sup>3</sup>Department of Geology, University of Maryland, College Park, Maryland, USA.

<sup>4</sup>Center for Advanced Radiation Sources, University of Chicago, Chicago, Illinois, USA.

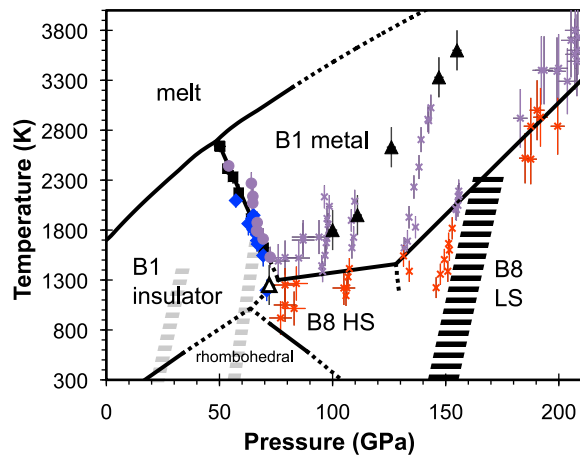


**Figure 1.** Phase diagram of wüstite, with comparison to electrical resistivity measurements. Melting curve: *Fischer and Campbell* [2010]. B1 insulator/metal: this study. B1/rhombohedral and rhombohedral/B8: *Fei and Mao* [1994]. B1/B8: *Fischer et al.* [2011], *Kondo et al.* [2004], and *Ozawa et al.* [2010a]. B8 HS/LS: *Ozawa et al.* [2010b]. Proposed phase boundaries are shown in black, with dashed portions representing shock resistivity data along the Hugoniot [*Knittle et al.*, 1986]. Solid triangles: metallic phase, open triangle: partial conversion from insulator to metallic phase. Shaded regions: approximate  $P$ - $T$  conditions of diamond cell resistivity measurements from *Ohta et al.* [2010]. Grey shaded regions: semi-conductor. Black shaded region: metallic. Crosses: XRD data from *Kondo et al.* [2004] (75–95 GPa), *Fischer et al.* [2011] (95–160 GPa), and *Ozawa et al.* [2010a] (180–210 GPa). Purple crosses: B1 structure. Red-orange crosses: B8 structure.

[2010]. Powdered  $\text{Fe}_{0.94}\text{O}$  was loaded as a pressed foil into a diamond anvil cell with a steel gasket, with argon as the pressure medium and thermal insulator and ruby powder as the pressure standard [*Mao et al.*, 1986]. Reported pressures are an average of pressure measurements collected at multiple ruby markers within the sample chamber both before and after heating, with an estimated thermal pressure contribution of 2.5 GPa added to the measured value [*Dewaele et al.*, 2007]. Errors in pressure are estimated as  $1\sigma$  uncertainties of the measured pressure, with an additional uncertainty of 1 GPa added to account for uncertainty in the thermal pressure component.

[6] After pressurization, samples were heated from one side with a 1064 nm Yb-doped fiber laser. Laser power was increased gradually and several temperature measurements were made at each laser power. Samples were heated in 1–4 locations, with each spot heated only once. Temperature distributions were measured by multispectral imaging radiometry [*Campbell*, 2008], allowing construction of the emissivity and temperature distributions in the hot spot in two dimensions.

[7] Figure 2 illustrates temperature-dependent variations in emissivity. A phase change was identified by discontinuities in temperature-emissivity profiles across the central region of the hot spot (Figure 2), reflecting changes in the sample’s optical (and possibly thermal transport) properties through a phase transition [*Campbell*, 2008]. The observed increase in emissivity indicates a transition and a

‘darkening’ of the sample, though detailed information about the nature of the optical transition cannot be extracted from these graybody emissivity measurements. For each experiment the temperature-emissivity discontinuities were identified in multiple temperature maps, at different laser powers. Each reported temperature is a mean calculated from 3–6 temperature maps, and from 3–7 distinct temperature-emissivity profiles across each map. Errors in temperature are one standard deviation of these values.

[8] High pressure, high temperature X-ray diffraction experiments were performed at Sector 13-ID-D (GSECARS) of the Advanced Photon Source, Argonne National Laboratory [*Prakapenka et al.*, 2008; *Shen et al.*, 2005]. Methods for the X-ray diffraction experiments are similar to those described by *Fischer et al.* [2011]. Samples were pressed foils of  $\text{Fe}_{0.94}\text{O}$ ,  $\text{Fe}_{0.94}\text{O} + \text{Fe}$  (1:1.23 by mass), or  $\text{Fe}_{0.94}\text{O} + \text{Fe}_3\text{O}_4$  (~1.5:1 by volume) powders to generate samples with different wüstite stoichiometries. Mixing wüstite with metallic Fe ensures that the oxide was saturated in iron, and presumably stoichiometric, at high pressures and temperatures [*Campbell et al.*, 2009; *Fischer et al.*, 2011; *Seagle et al.*, 2008; *Stølen and Grønbold*, 1996]. We assume that equilibrating wüstite with magnetite similarly has the effect of reducing the stoichiometry of the wüstite. The precise stoichiometry of our samples is not critical, but we attempt to vary the initial stoichiometry to investigate its effects on the observed phase transition.

[9] Samples were loaded into diamond anvil cells in a rhenium gasket between layers of NaCl, which served as the pressure medium, thermal insulator, and pressure standard, using its thermal equation of state [*Fei et al.*, 2007]. In using the pressure medium as the pressure standard, we correct its temperature to account for an axial thermal gradient [*Campbell et al.*, 2009]. Angle-dispersive X-ray diffraction experiments were performed using an X-ray beam ( $\lambda = 0.3344 \text{ \AA}$ ) measuring  $5 \mu\text{m} \times 5 \mu\text{m}$ . The sample was compressed and laser-heated from each side by  $1.064 \mu\text{m}$  Yb fiber lasers with ‘flat top’ profiles [*Prakapenka et al.*, 2008], while the diamond cell was water-cooled. Patterns

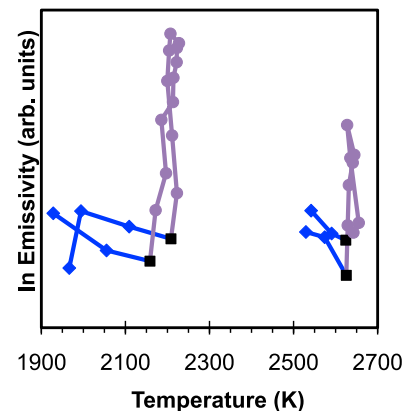


**Figure 2.** Temperature-emissivity profiles across the center of laser-heated spots at 59 GPa (left profiles) and 50 GPa (right profiles). The discontinuous increase in emissivity (black squares) corresponds to metallization. Blue diamonds: low emissivity (insulator) phase; purple circles: high emissivity (metallic) phase. The emissivity units are arbitrary, but full scale is 1.8 natural log units.

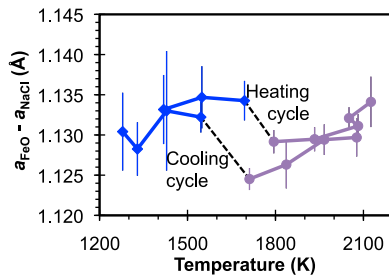


**Figure 3.** Lattice parameter of wüstite (relative to NaCl, to account for pressure variations) as a function of temperature during heating and cooling at 65–70 GPa. The discontinuous change in lattice parameter with temperature at 1600–1800 K (dashed lines) corresponds to metallization. Blue diamonds: low density (insulator) phase; purple circles: high density (metallic) phase. Typical uncertainty in sample temperature is  $\sim 100$  K.

were collected on heating and cooling. Temperatures were determined spectroradiometrically [Heinz and Jeanloz, 1987], and were measured during the collection of each diffraction pattern. The laser-heated spots were much larger than the X-ray beam to minimize radial temperature gradients. Some temperature measurements used in this study were recorded only on the upstream side of the sample, because of technical difficulties with measurements on the downstream side during one set of experiments. Temperatures were measured from a region  $5 \mu\text{m}$  in diameter in the center of the laser-heated spot, comparable in size to the area probed by the X-rays. The X-rayed region was  $\sim 4 \pm 1 \mu\text{m}$  in diameter (FWHM), much smaller than the laser-heated spot (diameter of  $\sim 20\text{--}30 \mu\text{m}$ ) to minimize radial temperature gradients. Formation of  $\text{Fe}_3\text{C}$  was observed in some of the experiments [Prakapenka et al., 2003]. Temperatures measured on the surface of the sample were corrected downward by 3% to account for an axial temperature gradient [Campbell et al., 2007, 2009].

### 3. Results

[10] Using the radiometric technique, discontinuities in temperature-emissivity profiles across the hot spot, interpreted as phase changes, were observed at 50–70 GPa. At this phase change, the effective emissivity of the sample greatly increases, consistent with metallization. Pressures and temperatures at which this phase transition are observed radiometrically are reported in Table S1 in the auxiliary material.<sup>1</sup>

[11] To detect the small changes in sample volume indicative of this phase transition, we plotted the difference between the lattice parameters of wüstite and NaCl ( $a_{\text{FeO}} - a_{\text{NaCl}}$ ) as a function of sample temperature (Figure 3). Lattice parameters increase monotonically with heating as the sample experiences thermal expansion; however, in these experiments, changes in thermal pressure make it difficult to interpret variations in a single lattice parameter. The difference between the lattice parameters of two materials during heating may increase, decrease, or remain constant

during heating, depending on the thermal expansions of the materials, but this difference will follow a continuous trend when neither material undergoes a phase transition. In these experiments, we observed a sudden discontinuous drop in the quantity  $a_{\text{FeO}} - a_{\text{NaCl}}$  across the radiometrically-determined phase boundary (Table S2). This cannot be due to a sudden increase in the lattice parameter of NaCl, because it has no known phase transition in this  $P$ - $T$  range and because NaCl was not used as the pressure medium in the radiometric experiments; therefore it must indicate a drop in the lattice parameter of FeO. We conclude that the phase change in FeO is isostructural, because its observed diffraction peaks indicated the B1 structure throughout these experiments. This method explicitly incorporates changes in pressure across the phase transition through the use of the lattice parameter of the pressure standard, so that the volume change must be due to the transition only, as long as the sample and pressure medium maintain mechanical equilibrium. The volume of FeO drops with increasing temperature (the opposite of what would be expected from thermal expansion), consistent with a transition to a higher-pressure phase with a negative Clapeyron slope. The weighted average of volume changes across the transition is  $0.39 \pm 0.05\%$ , after small corrections for changes in pressure and temperature with each crossing. Jeanloz and Ahrens [1980] reported a transition with  $\Delta V$  of 4%, but we now recognize (Figure 1) that the Hugoniot passes through multiple phase transitions, making the shock data difficult to interpret.

[12] The data from the radiometric technique and the brackets on the metal-insulator transition from X-ray diffraction are shown in Figure 4. Data points from samples with varying stoichiometry all fall along the same line, indicating that this phase transition is independent of stoichiometry within the resolution of our measurements. A data point from shock experiments in which resistivity was

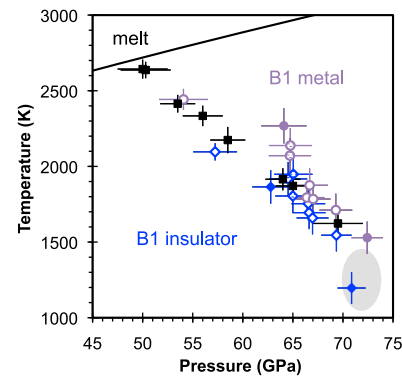


**Figure 4.** The proposed metallization phase boundary. Black squares correspond to pressures and temperatures of a sudden increase in sample emissivity from radiometric techniques. Blue diamonds and purple circles correspond to lower and upper bounds, respectively, of the volume drop in wüstite measured by X-ray diffraction. Filled symbols:  $\text{Fe}_{0.94}\text{O}$ . Open symbols:  $\text{Fe}_{0.94}\text{O}$  coexisting with Fe. Shaded symbols:  $\text{Fe}_{0.94}\text{O}$  coexisting with  $\text{Fe}_3\text{O}_4$ . Shaded ellipse: partial conversion to the metallic phase from shocked resistivity measurements [Knittle et al., 1986]. Black line: melting curve [Fischer and Campbell, 2010].

<sup>1</sup>Auxiliary materials are available in the HTML. doi:10.1029/2011GL049800.

measured directly [Knittle *et al.*, 1986], showing a partial conversion to metal, is consistent with our data.

#### 4. Discussion

[13] The proposed overall phase diagram for wüstite is shown in Figures 1 and S1, incorporating phase boundaries determined from several previous studies [Fei and Mao, 1994; Fischer and Campbell, 2010; Fischer *et al.*, 2011; Kondo *et al.*, 2004; Ozawa *et al.*, 2010a, 2010b], in addition to the insulator-metal B1 boundary reported here. Figure 1 illustrates the thermodynamic necessity of this transition: no B1/B8/rhombohedral triple point can be drawn based on the earlier B1/B8 data that does not violate Schreinemaker's rules [Zen, 1966], indicating the presence of another phase boundary in this  $P$ - $T$  region. Furthermore, the metallization observed in earlier electrical resistivity experiments [Knittle and Jeanloz, 1991; Knittle *et al.*, 1986] does not coincide with the B1/B8 boundary [Fischer *et al.*, 2011; Kondo *et al.*, 2004; Ozawa *et al.*, 2010a]. Shock resistivity measurements along the Hugoniot [Knittle *et al.*, 1986] fall entirely within the B1 stability field in the pressure range of metallization (Figure 1). Therefore earlier measurements of shocked metallic FeO [Knittle *et al.*, 1986] must have been made on B1 FeO, requiring the presence of an isostructural insulator-metal transition as reported here. Our new phase boundary is consistent with earlier measurements on the resistivity of FeO [Knittle *et al.*, 1986; Ohta *et al.*, 2010] (Figure 1).

[14] Metallization of FeO at high pressures has implications for the stability of (Mg,Fe)O in the Earth's lower mantle. There will not be a complete solid solution in ferropericlase between insulating and conducting endmembers, though the extent of the solid solution and the width of the compositional gap are unknown. In FeO-rich regions such as those proposed to exist in pockets at the core-mantle boundary (CMB) [Wicks *et al.*, 2010], ferropericlase may break down into two phases, an insulating Fe-poor phase and a metallic Fe-rich phase. This may have been undetected in most previous X-ray diffraction studies of ferropericlase due to the use of MgO-rich starting compositions that allow solid solution with FeO, or a narrow compositional gap that produces ferropericlases with similar compositions, so that the splitting of (Mg,Fe)O peaks is too small to resolve. This immiscibility gap may explain the dissociation of magnesiowüstite into magnesium-rich and iron-rich components reported in a previous study [Dubrovinsky *et al.*, 2000].

[15] The presence of FeO-rich regions along the CMB will increase the temperature in the  $D''$  layer due to the higher thermal conductivity of metallic FeO, and variations in the thickness of FeO-rich regions will produce lateral temperature variations of up to several hundred K [Manga and Jeanloz, 1996]. Higher temperatures increase the likelihood of stabilizing the post-perovskite phase, and also favors a double-crossing, with perovskite becoming stable again at the CMB [Hernlund *et al.*, 2005].

[16] Forced nutations of the Earth exhibit anomalous dissipation, which can be explained as ohmic dissipation resulting from magnetic field coupling at the CMB if the base of the mantle contains a layer with metallic electrical conductivity [Buffett, 1992; Buffett and Christensen, 2007; Buffett *et al.*, 2000]. An enrichment in FeO in this layer could account for this increased conductivity. Additionally, the liquid immiscibility field in the Fe-O system contracts with

increasing pressure [Ringwood and Hibberson, 1990], with melting occurring as a simple eutectic by 50 GPa [Seagle *et al.*, 2008]. This evolution toward a single metallic liquid at high pressures can be explained by the Fe-O bond becoming more metallic with increasing pressure, allowing oxygen to more easily dissolve into the metallic melt.

[17] Finally, the existence of a metallic phase of FeO will slightly alter the equation of state parameters reported for B1 FeO [Fischer *et al.*, 2011], since earlier equations of state incorporated  $P$ - $V$ - $T$  data on both insulating and metallic phases. However, since the volume change of this transition is small, its effect is confined to the  $P$ - $T$  region near the phase boundary. A comparison of fitted equation of state parameters for the metallic and insulating phases versus a fit including both B1 phases is shown in Table S3. The metal-insulator phase boundary should also produce a kink in the melting curve of wüstite, but it should again be subtle due to the small volume change. Such a change in slope was likely undetectable in previous measurements of the melting curve [Fischer and Campbell, 2010]. Gramsch *et al.* [2003] predicted metallization of B1 FeO at 110 GPa and 0 K with a volume change of  $-0.3\%$ , in agreement with our findings.

[18] **Acknowledgments.** Portions of this work were performed at GeoSoilEnviroCARS (Sector 13), Advanced Photon Source (APS), Argonne National Laboratory. GeoSoilEnviroCARS is supported by the National Science Foundation - Earth Sciences (EAR-0622171) and Department of Energy - Geosciences (DE-FG02-94ER14466). Use of the Advanced Photon Source was supported by the U. S. Department of Energy, Office of Science, Office of Basic Energy Sciences, under contract DE-AC02-06CH11357. This material is based upon work supported by a National Science Foundation Graduate Research Fellowship to R.A.F. This work was also supported by the National Science Foundation by grant EAR-0847217 to A.J.C.

[19] The editor thanks the two anonymous reviewers.

#### References

- Buffett, B. A. (1992), Constraints on magnetic energy and mantle conductivity from the forced nutations of the Earth, *J. Geophys. Res.*, *97*, 19,581–19,597, doi:10.1029/92JB00977.
- Buffett, B. A., and U. R. Christensen (2007), Magnetic and viscous coupling at the core-mantle boundary: Inferences from observations of the Earth's nutations, *Geophys. J. Int.*, *171*, 145–152, doi:10.1111/j.1365-246X.2007.03543.x.
- Buffett, B. A., E. J. Garnero, and R. Jeanloz (2000), Sediments at the top of Earth's core, *Science*, *290*, 1338–1342, doi:10.1126/science.290.5495.1338.
- Campbell, A. J. (2008), Measurement of temperature distributions across laser-heated samples by multispectral imaging radiometry, *Rev. Sci. Instrum.*, *79*, 015108, doi:10.1063/1.2827513.
- Campbell, A. J., C. T. Seagle, D. L. Heinz, G. Shen, and V. B. Prakapenka (2007), Partial melting in the iron-sulfur system at high pressure: A synchrotron X-ray diffraction study, *Phys. Earth Planet. Inter.*, *162*, 119–128, doi:10.1016/j.pepi.2007.04.001.
- Campbell, A. J., L. Danielson, K. Richter, C. T. Seagle, Y. Wang, and V. B. Prakapenka (2009), High pressure effects on the iron-iron oxide and nickel-nickel oxide oxygen fugacity buffers, *Earth Planet. Sci. Lett.*, *286*, 556–564, doi:10.1016/j.epsl.2009.07.022.
- Dewaele, A., M. Mezouar, N. Guignot, and P. Loubeyre (2007), Melting of lead under high pressure studied using second-scale time-resolved x-ray diffraction, *Phys. Rev. B*, *76*, 144106, doi:10.1103/PhysRevB.76.144106.
- Dubrovinsky, L. S., N. A. Dubrovinskaia, S. K. Saxena, H. Annersten, E. Hälenius, H. Harryson, F. Tutti, S. Rekhi, and T. Le Bihan (2000), Stability of ferropericlase in the lower mantle, *Science*, *289*, 430–432, doi:10.1126/science.289.5478.430.
- Fei, Y., and H. Mao (1994), In-situ determination of the NiAs phase of FeO at high-pressure and temperature, *Science*, *266*, 1678–1680, doi:10.1126/science.266.5191.1678.
- Fei, Y., A. Riccolleau, M. Frank, K. Mibe, G. Shen, and V. Prakapenka (2007), Toward an internally consistent pressure scale, *Proc. Natl. Acad. Sci. U. S. A.*, *104*, 9182–9186, doi:10.1073/pnas.0609013104.
- Fischer, R. A., and A. J. Campbell (2010), High-pressure melting of wüstite, *Am. Mineral.*, *95*, 1473–1477, doi:10.2138/am.2010.3463.



- Gramsch, S. A., R. E. Cohen, and S. Y. Savrasov (2003), Structure, metal-insulator transitions, and magnetic properties of FeO at high pressures, *Am. Mineral.*, *88*, 257–261.
- Fischer, R. A., A. J. Campbell, G. A. Shofner, O. T. Lord, P. Dera, and V. B. Prakapenka (2011), Equation of state and phase diagram of FeO, *Earth Planet. Sci. Lett.*, *304*, 496–502, doi:10.1016/j.epsl.2011.02.025.
- Heinz, D. L., and R. Jeanloz (1987), Temperature measurement in the laser-heated diamond anvil cell, in *High-Pressure Research in Mineral Physics*, edited by M. H. Manghni and Y. Syono, pp. 113–127, Terra Sci., Tokyo.
- Hernlund, J. W., C. Thomas, and P. J. Tackley (2005), A doubling of the post-perovskite phase boundary and structure of the Earth's lowermost mantle, *Nature*, *434*, 882–886, doi:10.1038/nature03472.
- Jeanloz, R., and T. J. Ahrens (1980), Equations of state of FeO and CaO, *Geophys. J. R. Astron. Soc.*, *62*, 505–528.
- Kantor, I., A. Kurnosov, C. McCammon, and L. Dubrovinsky (2008), Monoclinic FeO at high pressures, *Z. Kristallogr.*, *223*, 461–464, doi:10.1524/zkri.2008.0049.
- Knittle, E., and R. Jeanloz (1991), The high-pressure phase diagram of Fe<sub>0.94</sub>O: A possible constituent of the Earth's core, *J. Geophys. Res.*, *96*, 16,169–16,180, doi:10.1029/90JB00653.
- Knittle, E., R. Jeanloz, A. C. Mitchell, and W. J. Nellis (1986), Metallization of Fe<sub>0.94</sub>O at elevated pressures and temperatures observed by shock-wave electrical resistivity measurements, *Solid State Commun.*, *59*, 513–515, doi:10.1016/0038-1098(86)90699-X.
- Kondo, T., E. Ohtani, N. Hirao, T. Yagi, and T. Kikegawa (2004), Phase transitions of (Mg,Fe)O at megabar pressures, *Phys. Earth Planet. Inter.*, *143–144*, 201–213, doi:10.1016/j.pepi.2003.10.008.
- Manga, M., and R. Jeanloz (1996), Implications of a metal-bearing chemical boundary layer in D' for mantle dynamics, *Geophys. Res. Lett.*, *23*, 3091–3094, doi:10.1029/96GL03021.
- Mao, H., J. Xu, and P. M. Bell (1986), Calibration of the ruby pressure gauge to 800 kbar under quasi-hydrostatic conditions, *J. Geophys. Res.*, *91*, 4673–4676, doi:10.1029/JB091iB05p04673.
- Mao, H., J. Shu, Y. Fei, J. Hu, and R. J. Hemley (1996), The wüstite enigma, *Phys. Earth Planet. Inter.*, *96*, 135–145, doi:10.1016/0031-9201(96)03146-9.
- McDonough, W. F. (2003), Compositional model for the Earth's core, in *Treatise of Geochemistry*, vol. 2, *The Mantle and Core*, edited by R. W. Carlson, pp. 547–568, Elsevier, Oxford, U. K., doi:10.1016/B0-08-043751-6/02015-6.
- Murakami, M., K. Hirose, S. Ono, T. Tsuchiya, M. Isshiki, and T. Watanuki (2004), High pressure and high temperature phase transitions of FeO, *Phys. Earth Planet. Inter.*, *146*, 273–282, doi:10.1016/j.pepi.2003.06.011.
- Ohta, K., K. Hirose, K. Shimizu, and Y. Ohishi (2010), High-pressure experimental evidence for metal FeO with normal NiAs-type structure, *Phys. Rev. B*, *82*, 174120, doi:10.1103/PhysRevB.82.174120.
- Ozawa, H., K. Hirose, S. Tateno, N. Sata, and Y. Ohishi (2010a), Phase transition boundary between B1 and B8 structures of FeO up to 210 GPa, *Phys. Earth Planet. Inter.*, *179*, 157–163, doi:10.1016/j.pepi.2009.11.005.
- Ozawa, H., K. Hirose, H. Ishii, N. Hiraoka, and Y. Ohishi (2010b), Spin transition of iron and crystal structure in FeO from X-ray emission spectroscopy and diffraction measurements, Abstract MR23A-2010 presented at 2010 Fall Meeting, AGU, San Francisco, Calif., 13–17 Dec.
- Prakapenka, V. B., G. Shen, and L. S. Dubrovinsky (2003), Carbon transport in diamond anvil cell, *High Temp. High Pressures*, *35/36*, 237–249, doi:10.1068/hjtr098.
- Prakapenka, V. B., A. Kubo, A. Kuznetsov, A. Laskin, O. Shkurikhin, P. Dera, M. L. Rivers, and S. R. Sutton (2008), Advanced flat top laser heating system for high pressure research at GSECARS: Application to the melting behavior of germanium, *High Pressure Res.*, *28*, 225–235, doi:10.1080/08957950802050718.
- Ringwood, A. E. (1977), Composition of the core and implications for origin of the earth, *Geochem. J.*, *11*, 111–135, doi:10.2343/geochemj.11.111.
- Ringwood, A. E., and W. Hibberson (1990), The system Fe-FeO revisited, *Phys. Chem. Miner.*, *17*, 313–319, doi:10.1007/BF00200126.
- Seagle, C. T., D. L. Heinz, A. J. Campbell, V. B. Prakapenka, and S. T. Wanless (2008), Melting and thermal expansion in the Fe-FeO system at high pressure, *Earth Planet. Sci. Lett.*, *265*, 655–665, doi:10.1016/j.epsl.2007.11.004.
- Shen, G., M. L. Rivers, Y. Wang, and S. R. Sutton (2005), Facilities for high-pressure research with the diamond anvil cell at GSECARS, *J. Synchrotron Radiat.*, *12*, 642–649, doi:10.1107/S0909049505022442.
- Sherman, D. M. (1989), The nature of the pressure-induced metallization of FeO and its implications to the core-mantle boundary, *Geophys. Res. Lett.*, *16*, 515–518, doi:10.1029/GL016i006p00515.
- Stølen, S., and F. Grønvold (1996), Calculation of the phase boundaries of wüstite at high pressure, *J. Geophys. Res.*, *101*, 11,531–11,540, doi:10.1029/96JB00524.
- Struzhkin, V. V., H.-k. Mao, J. Hu, M. Schwoerer-Böhning, J. Shu, and R. J. Hemley (2001), Nuclear inelastic X-ray scattering of FeO to 48 GPa, *Phys. Rev. Lett.*, *87*, 255501, doi:10.1103/PhysRevLett.87.255501.
- Wicks, J. K., J. M. Jackson, and W. Sturhahn (2010), Very low sound velocities in iron-rich (Mg,Fe)O: Implications for the core-mantle boundary region, *Geophys. Res. Lett.*, *37*, L15304, doi:10.1029/2010GL043689.
- Yagi, T., K. Fukuoka, H. Takei, and Y. Syono (1988), Shock compression of wüstite, *Geophys. Res. Lett.*, *15*, 816–819, doi:10.1029/GL015i008p00816.
- Zen, E.-A. (1966), Construction and pressure-temperature diagrams for multicomponent systems after the method of Schreinemakers geometric approach, *U.S. Geol. Surv. Bull.*, *1225*.

A. J. Campbell and R. A. Fischer, Department of the Geophysical Sciences, University of Chicago, 5734 S. Ellis Ave., Chicago, IL 60637, USA. (rfischer@uchicago.edu)

P. Dera and V. B. Prakapenka, Center for Advanced Radiation Sources, University of Chicago, 5640 S. Ellis Ave., Chicago, IL 60637, USA.

O. T. Lord, Department of Earth Sciences, University College London, Kathleen Lonsdale Building, Gower Street, London WC1E 6BT, UK.

G. A. Shofner, Department of Geology, University of Maryland, College Park, MD 20742, USA.